

Ultra-Low Crosstalk, Flat Pass-band and Low Loss CWDM (De-)Multiplexer based on PSO Algorithm

Xiang Liu

State Key Laboratory of Functional Materials for Informatics
Shanghai Institute of Microsystem and Information Technology,
Chinese Academy of Sciences
Shanghai, China
liuxiang@mail.sim.ac.cn

Yingxuan Zhao

State Key Laboratory of Functional Materials for Informatics
Shanghai Institute of Microsystem and Information Technology,
Chinese Academy of Sciences
Shanghai, China
zhaoyx@mail.sim.ac.cn

Abstract—We obtain an ultra-low crosstalk, flat pass-band (de-)multiplexer using PSO algorithm. The results show that the (de-)multiplexer achieves a pass-band flatness of 15 nm, a crosstalk below -33.4 dB and insertion loss below 0.2 dB.

Keywords—CWDM, (de-)multiplexer, PSO, Silicon photonics

I. INTRODUCTION

With the explosive growth of data communications, silicon photonics has led a rapid development in the field of information interconnection with its mature process manufacturing technology, faster data transmission speed and larger optical bandwidth [1]. To enhance the transmission capacity of data communications, one of the promising solutions is wavelength division multiplexing (WDM), which is proposed based on the silicon photonic platform [2]. The WDM technology allows multiple information-carrying wavelengths to be propagated in the same optical waveguide. However, WDM (de-)multiplexer requires a sufficiently large operational bandwidth for the individual channels and a low crosstalk to ensure sufficient stability and accuracy of data transmission [3]. The common O-band coarse wavelength division multiplexing (CWDM) technology offers a channel spacing of about 20nm, which corresponds to different wavelength centers of 1271nm, 1291nm, 1311nm and 1331nm [4]. The technology allows for reduced accuracy to the emission wavelength of the laser in optical communication networks, with greater robustness to external temperature variations. CWDM (de-)multiplexers implemented on a silicon photonic platform are more tolerant to precise temperature tuning and stringent fabrication process, which further reduces fabrication costs and energy loss [5]. Several common on-chip different silicon-based CWDM approaches have been proposed. Those based on finite impulse response (FIR) filter include array waveguide gratings (AWG), Bragg gratings and Mach-Zehnder interferometers (MZIs). AWG-based CWDM (de-)multiplexers exhibit low crosstalk, but their insertion loss and footprint are relatively large [6]. Bragg gratings are also a popular approach to implementing CWDM, with the main advantages of reduced dimensions and flat pass-band. However, the multiplexer is prone to high crosstalk due to the adoption of Bragg gratings [7]. CWDM (de-)multiplexers based on the MZI structure offer simple fabrication process and low loss, but the robustness to channel crosstalk needs to be improved [8]. Infinite impulse response (IIR) filter are available as micro-ring resonators (MRRs). MRRs provide small footprint and low loss, but have a poor pass-band and are subject to center wavelength drift [9].

In this paper, we propose a novel O-band 4-channel CWDM (de-)multiplexer based on MZI structure using particle swarm optimization (PSO) algorithm. Simulation

results show that the (de-)multiplexer exhibits an average 1dB pass-band of 15 nm, low crosstalk of less than -33.4 dB, and low loss of less than 0.2 dB.

II. DEVICE DESIGN

The proposed CWDM (de-)multiplexer is achieved based on a cascaded MZI structure. Within a given free spectral range (FSR), we design different cascaded MZI filters to maximize the flat-top pass-band. Prior to the design, we need to determine the FSR and the channel spacing (CS) of the multiplexer. The FSR of an individual MZI structure is inversely related to the delay line length and is generally defined as $FSR = \lambda_c^2 / (n_g \cdot \Delta L)$. Where λ_c represents the central wavelength of the operating band, n_g refers to the group refractive index of the adopted waveguide in TE₀ mode, and ΔL refers to the physical path length difference between the two arms of the MZI structure. The (de-)multiplexer can be divided into two stages, as shown in Fig. 1(a), consisting of three cascaded MZI blocks. Each MZI block is designed as an interleaver. In the first stage, this block is assigned to divide the odd and even wavelength channels. The central wavelength is set at 1301 nm and the FSR is designed to be 40 nm. The output from the first interleaver will be transmitted to the two MZI blocks of the second stage. These two interleavers are intended to divide the wavelengths of the odd and even channels from the first stage into different channels, eventually generating four separate channels. As shown in Fig. 1b and Fig. 1c, they represent the specific interleaver for the first and second stages respectively.

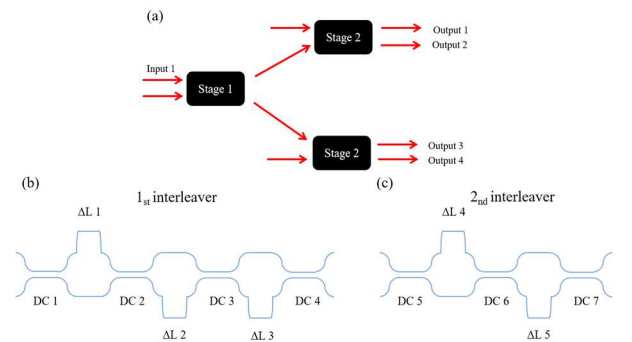


Fig.1. (a) The schematic layout of the proposed CWDM (de-)multiplexer. (b) The configuration of 1_{st} interleaver with three cascaded filters. (c) The configuration of 2_{nd} interleaver with two cascaded filters.

The first interleaver consists of three MZI blocks, while the second one is composed of two MZI blocks. In the design process, we can optimize the power splitting ratios and delay line length in each interleaver to achieve the tradeoff of pass-band flatness and crosstalk. In terms of design principles, we can employ the transfer matrix method to simulate the optical propagation of the entire CWDM (de-)multiplexer. One of the

MZI block involves a phase shift of π , which is implemented by extending the delay length to adjust the central wavelength of the different channels. This phase shift length can be defined as $L_\pi = \lambda_c / (2 \cdot n_{\text{eff}})$, where n_{eff} is the effective refractive index of the waveguide in TE₀ mode at a wavelength of λ_c . In the second stage of the interleaver, a phase shift of $\pi/2$ needs to be achieved for one of the odd or even channels, which is based on a similar calculation. The (de-)multiplexer is modelled by means of transfer matrix method where several parameters of the transfer matrix can be optimized to obtain large pass-band flatness and low crosstalk using particle swarm optimization algorithms. The device is implemented on a standard SOI platform and is compatible with conventional CMOS processes. The 200 mm SOI wafers with a top silicon layer of 220 nm, a buried oxygen layer of 2 μm is selected to be compatible with the standard fabrication process. A standard SiO₂ top cladding is applied in this device. The CWDM (de-)multiplexer is designed for TE mode. The width of the waveguide is set to 350 nm to ensure that no mode conversion occurs when the optical mode propagates.

III. OPTIMIZATION FUNCTION AND ALGORITHM

When optimizing the configuration of CWDM (de-)multiplexers, the labor and time investment can be considerable compared to the traditional manual adjustment method. By using intelligent optimization algorithms to help with the design, we can both improve the accuracy of the optimization objectives and reduce unnecessary labor. In this paper, for a multi-objective simultaneous optimization task such as CWDM, we employ a PSO algorithm to carry out the design. The PSO algorithm models the behavior of a flock of birds searching for food. Particle swarms have the property of sharing and iterating information when searching for targets. Compared to other optimization algorithms, the particle swarm algorithm is able to perform a tradeoff of convergence speed and accuracy. as shown in equations 1-3, the mathematical model of the PSO algorithm can be expressed as:

$$v_{i,t+1}^d = \omega v_{i,t}^d \text{rand} + c_1 \text{rand}(p_{i,t}^d - x_{i,t}^d) + c_2 \text{rand}(p_{g,t}^d - x_{i,t}^d) \quad (1)$$

$$x_{i,t+1}^d = x_{i,t}^d + v_{i,t+1}^d \quad (2)$$

$$\omega = \omega_{\text{max}} - \frac{t(\omega_{\text{max}} - \omega_{\text{min}})}{G} \quad (3)$$

We define a D-dimensional variable space in which the position, velocity, individual optimal position and global optimal position of the particle are represented as follows:

$$X_i = (x_{i1}, x_{i2}, x_{i3}, \dots, x_{id}, \dots, x_{iD}) \quad (4)$$

$$V_i = (v_{i1}, v_{i2}, v_{i3}, \dots, v_{id}, \dots, v_{iD}) \quad (5)$$

$$P_i = (p_{i1}, p_{i2}, p_{i3}, \dots, p_{id}, \dots, p_{iD}) \quad (6)$$

$$P_g = (p_{g1}, p_{g2}, p_{g3}, \dots, p_{gd}, \dots, p_{gD}) \quad (7)$$

In the above equations, i , t , G represent the i -th particle, the t -th iteration and the total number of iterations, respectively. ω , c_1 , c_2 represent the inertial, social and cognitive parameters, respectively. They are important control parameters in this algorithm and have a large impact on the convergence speed and robustness of the algorithm. Unlike the traditional PSO algorithm, this work introduces a variable inertia constant in order to further improve its robustness against falling into local traps. It will tailor the global search capability of the algorithm as the iteration progresses, helping to find the optimal value faster. The rand in equation 1 is a random number that takes values in the range from 0 to 1. The parameter settings for the PSO algorithm are shown in Table 1.

Table 1. Parameter settings for the PSO algorithm.

Symbol	Value	Symbol	Value
c1	1.2	Particle swarms	400
c2	1.4	T	20
ω_{max}	1	D	7
ω_{min}	0.4	rand	[0,1]

We plug the PSO algorithm into the computation of the transfer matrix of the CWDM (de-)multiplexer and define the figure-of-merit (FoM) as the evaluation function, as shown in equation 8.

$$FoM = \frac{\sum_{i=1}^N (\lambda_{s1}^{chi} - \lambda_{s2}^{chi}) + \sum_{i=1}^N (T_{chi} - T_{chi}')_{\text{min}}}{4FSR} \quad (8)$$

Where N represents the defined number of channels, λ_{s1}^{chi} and λ_{s2}^{chi} refer to the wavelengths on both sides of the channel corresponding to the 1 dB bandwidth respectively, and T_{ch} denotes the transmission under a certain channel. To better demonstrate the process of PSO algorithm optimization, the flow chart of the algorithm is presented in Fig. 1. The process will be automatically terminated when the algorithm obtains the optimal quality factor or at the end of the full iteration.

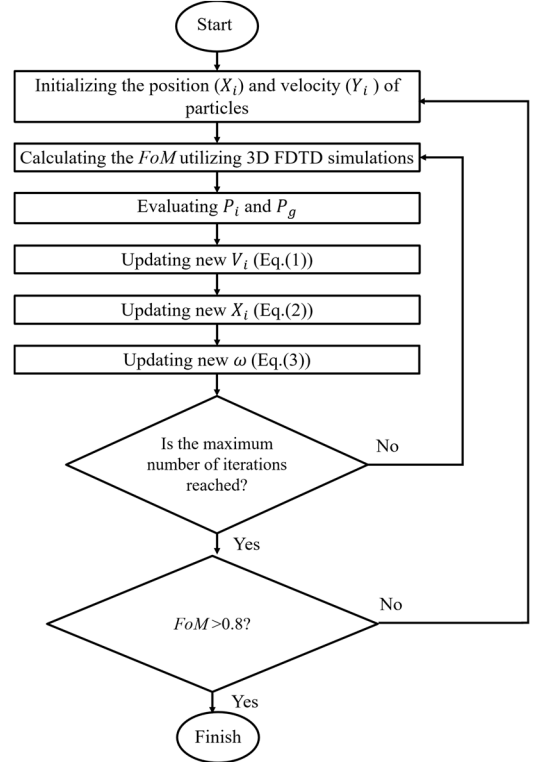


Fig.2. Flow chart of PSO algorithm.

IV. SIMULATION RESULTS AND DISCUSSION

We adopt the PSO algorithm to optimize the configuration of the CWDM (de-)multiplexer including the power splitting ratio and delay line length, based on the calculation of the transfer matrix. After the optimal configuration has been found, the results will be verified by Lumerical 3D FDTD. The device mainly works on O-band, covering the wavelength range from 1260 to 1340 nm. The (de-)multiplexer is achieved based on the TE fundamental mode. As shown in Fig. 3, the FoM convergence plot is shown here. It can be seen that the FoM gradually stabilizes at a minimum value of 0.81 after 9 iterations and remains stable during the subsequent searches.

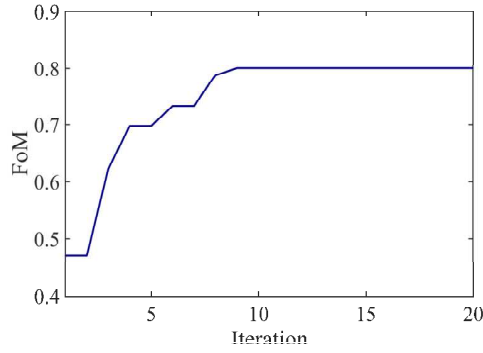


Fig.3 FoM variation curve of the device at each iteration.

Under the optimal results, the power splitters of first interleaver are configured as 0.5, 0.15, 0.24, 0.02 and the length differences are 9.59 μm , 19.19 μm and 19.48 μm respectively. The corresponding transmission plot is shown in Fig. 4. a. The interleaver A of the second stage has a coupling ratio configuration of 0.5, 0.26, 0.06 and length differences of 4.65 μm , and 9.30 μm respectively. The optimal configuration of the coupling ratio for interleaver B is 0.5, 0.26 and 0.06, and length differences are 4.79 μm and 9.58 μm . The transmission plot of the second stage interleavers A and B are shown in Fig. 4. b-c. The spectra of the completed CWDM (de-)multiplexer is shown in Fig. 5.

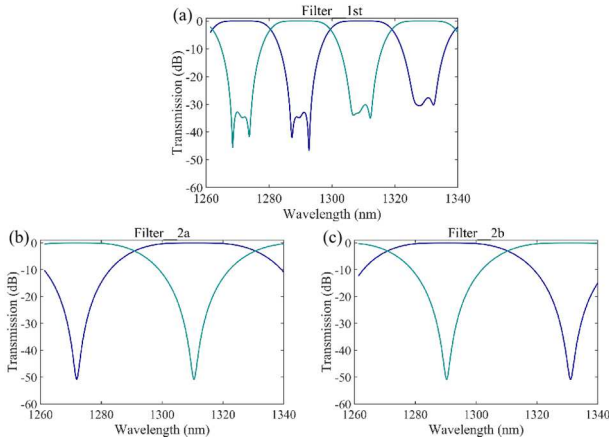


Fig. 4. Calculated transmission spectra of the 1st and 2nd interleaver.

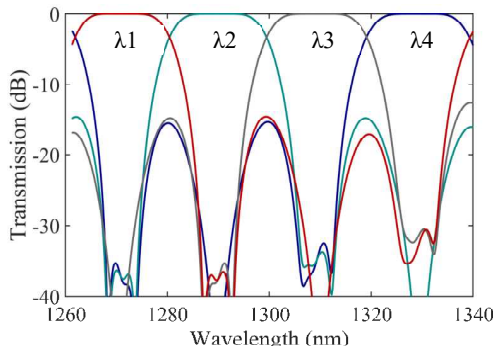


Fig. 5. Calculated transmission spectra of the completed (de-)multiplexer.

This device has a favorable flat-top pass-band and its average operational bandwidth for each channel reaches 15 nm. In addition, the channel crosstalk of the device is optimized, with

the average crosstalk of each channel below -33.4 dB. This indicates that our optimized (de-)multiplexer achieves a large operational bandwidth and ultra-low crosstalk. In addition, We also examined the insertion loss, which was less than 0.2 dB for each channel. our proposed (de-)multiplexer can better meet the requirements of CWDM, helping to enhance the data transmission capacity and improve its stability.

V. CONCLUSION

We propose an O-band CWDM (de-)multiplexer with large operational bandwidth, ultra-low channel crosstalk and low loss based on the PSO algorithm. Under the optimal configuration, the average operational bandwidth of each channel can reach more than 15 nm, the average crosstalk can be less than -33.4 dB, and the loss is less than 0.2 dB. The CWDM (de-)multiplexer, based on the optimization algorithm, can better meet the requirements for high-capacity data transmission.

ACKNOWLEDGMENT

This work is supported by National Key Research and Development Program of China [2022YFB2803100]; National major scientific research instrument development project [22127901]; Shanghai Sailing Program [22YF1456700].

REFERENCES

- [1] Pitris S, Moralis-Pegios M, Alexoudi T, et al. O-band silicon photonic transmitters for datacom and computer interconnects[J]. Journal of Lightwave Technology, 2019, 37(19): 5140-5148.
- [2] Dong P. Silicon photonic integrated circuits for wavelength-division multiplexing applications[J]. IEEE Journal of Selected Topics in Quantum Electronics, 2016, 22(6): 370-378.
- [3] Xu H, Shi Y. Flat-top CWDM (de) multiplexer based on MZI with bent directional couplers[J]. IEEE Photonics Technology Letters, 2017, 30(2): 169-172.
- [4] Dwivedi S, De Heyn P, Absil P, et al. Coarse wavelength division multiplexer on silicon-on-insulator for 100 GbE[C]/2015 IEEE 12th International Conference on Group IV Photonics (GFP). IEEE, 2015: 9-10.
- [5] Horst F, Green W M J, Assefa S, et al. Cascaded Mach-Zehnder wavelength filters in silicon photonics for low loss and flat pass-band WDM (de-) multiplexing[J]. Optics express, 2013, 21(10): 11652-11658.
- [6] Pan P, An J, Wang Y, et al. Compact 4-channel AWGs for CWDM and LAN WDM in data center monolithic applications[J]. Optics & Laser Technology, 2015, 75: 177-181.
- [7] Shi W, Yun H, Lin C, et al. Ultra-compact, flat-top demultiplexer using anti-reflection contra-directional couplers for CWDM networks on silicon[J]. Optics express, 2013, 21(6): 6733-6738.
- [8] Jeong S H, Shimura D, Simoyama T, et al. Si-nanowire-based multistage delayed Mach-Zehnder interferometer optical MUX/DeMUX fabricated by an ArF-immersion lithography process on a 300 mm SOI wafer[J]. Optics letters, 2014, 39(13): 3702-3705.
- [9] De Heyn P, De Coster J, Verheyen P, et al. Fabrication-tolerant four-channel wavelength-division-multiplexing filter based on collectively tuned Si microrings[J]. Journal of lightwave technology, 2013, 31(16): 3085-3092.